Influence of a Lightning Rod on the Bearing Accuracy of a Direction Finding System

Thomas Kaufmann*, Olivier Progin†, Christophe Fumeaux*
*School of Electrical and Electronic Engineering, The University of Adelaide, Adelaide SA 5005, Australia
†armasuisse, Wissenschaft und Technologie, Feuerwerkerstrasse 39, 3606 Thun, Switzerland
Corresponding Email: thomaska@eleceng.adelaide.edu.au

***Abstract*—Direction finding systems based on amplitude-comparison algorithms are commonly used today due to their simplicity and robustness. In order to protect the physical structure from lightning strikes, proper lightning protection must be applied. In many cases, due to the complexity of such a system, an internal lightning rod is not feasible. Placed externally, the metal rod influences the antenna patterns and ultimately deteriorates the detection quality of the whole system. In this paper, an analytical model is developed based on the Mie scattering of a perfect conducting cylinder to estimate an affected antenna pattern. Measurements confirm the validity of the analytical model. The impact on the overall bearing error is evaluated for different configurations of the system, and explain the significant errors for practical settings.**

***Keywords*-direction of arrival estimation, Mie scattering, lightning protection**

I. Introduction

Direction finding (DF) systems are important tools for passive detection of microwave pulse emitters, e.g. radar signals from a moving object. These systems are relevant for electronic intelligence (ELINT) on modern battlefield scenarios [1]–[3], but can also be used for tracking emitters in emergency situations. A common implementation is a bearing algorithm that exploits received amplitude differences from a number of squinted receiving antennas [4]. Amplitude-based direction finding algorithms are often preferred to other systems due to their simplicity and robustness. Additionally, multiple pulses can be discriminated in a simpler way than with other methods [4].

In practical implementations, the receiving antennas are usually arranged in a cylindrical symmetrical fashion to achieve omnidirectional coverage. Spiral antennas are often deployed as receiving elements because of their nearly ideal circularly polarized Gaussian pattern, which is maintained over a large frequency bandwidth. A typical example is the cavity-backed Archimedean spiral antenna evaluated in [5].

Often the DF structures are combined with other types of ELINT systems and need to be placed in harsh environments such as mountainous regions to survey large areas. A proper lightning protection is crucial to ensure safe operation and to reduce the maintenance effort in regions difficult to access. A lightning rod is generally used to protect the equipment from lightning strikes. This lightning rod has to be placed in the vicinity of the structure, but because of the complexity of the setup, it is often impossible to integrate it inside the system. The placement of this metal rod is then a trade-off between maximizing the protection of the system (placement close to the structure) and minimizing the electromagnetic influence of the metal rod on the bearing accuracy of the system (placement far from the structure).

For precision evaluations of DF systems, non-deterministic factors, i.e. noise measures, are usually taken into account to estimate the bearing accuracy [6]. In this paper, the systematic error introduced due to the (deterministic) influence of the lightning rod is evaluated. More generally, this theory can be applied to characterize the effect of any metallic cylindrical object in the close vicinity of the DF system. In this approach the scattered fields of a metal cylinder are assumed to interfere with the impinging signal at each antenna. The Mie theory [7] provides the theoretical framework for the scattering properties of a lightning rod. Assuming far-field conditions, the superposition of the scattered field with the unperturbed isolated antenna pattern yields a distorted pattern as an analytical result. Measurements are used to confirm the validity of this model. For several configurations of the DF system, the bearing error is evaluated based on this distorted antenna pattern.

This work is based on evaluations on an existing system. For confidentiality reasons, practical validations and technical details about the system cannot be provided here, but it can be commented that a very good qualitative agreement between theoretically expected and measured values could be achieved.

The paper is structured as follows: first the detection of Direction-of-Arrival (DoA) based on amplitude differences is briefly reviewed. Then the theoretical framework for determining the influence of the lightning rod on the antenna pattern is provided and validated with measurements. Afterwards, the influence of this distorted pattern on the bearing accuracy as systematic measurement errors is discussed.

II. Direction of Arrival Detection

In the amplitude-difference based DoA detection algorithm considered here, the receiving spiral antennas are assumed to have a nearly Gaussian angular gain pattern. The detection algorithm is formulated in the practically important azimuthal plane, where the antennas are cylindrically arranged. For two antennas placed at a squint angle of Ψ_s, the received power

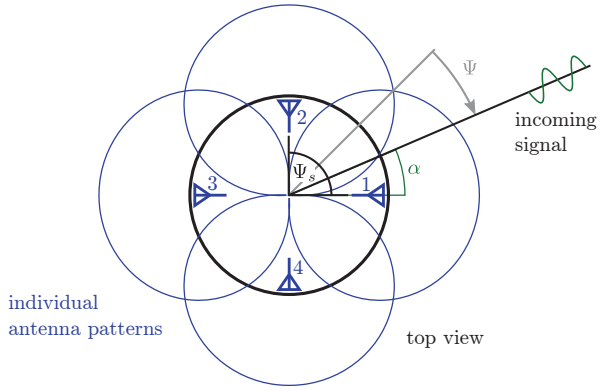

Fig. 1: Setup of a four element DF system with spiral antennas placed symmetrically around the structure.

is proportional to [4]

$$P_1 = e^{-K\left(\frac{\Psi_s/2+\Psi}{\Psi_0}\right)^2}, \quad P_2 = e^{-K\left(\frac{\Psi_s/2-\Psi}{\Psi_0}\right)^2} \tag{1}$$

with K a proportionality constant and Ψ_0 is half of the half-power beamwidth (HPBW). The geometrical setup of a four-antenna system is illustrated in Fig. 1. The angle of arrival Ψ measured from the beam crossover point between the two antennas is related to the angle of incidence α respective to antenna 1 as

$$\alpha = \Psi_s/2 - \Psi \tag{2}$$

Eventually the difference between the the received power in antenna 1 and antenna 2 in dB

$$R = 10 \log \frac{P_1}{P_2} \tag{3}$$

is easily found, for Gaussian antenna patterns, to be proportional to the angle of arrival

$$\Psi = \frac{\Psi_0^2 R}{20 K \Psi_s \log e}. \tag{4}$$

The angle of incidence is therefore detected in a straightforward fashion [4]. In a practical implementation of the system, usually a number of spiral antennas is employed to cover the whole azimuth. Considering that in such an assembly, each azimuthal section is covered by two antenna pairs, a linear weighting of the measured bearing angles for two antenna pairs is generally employed to minimize noise in the measurements.

It should be noted though, that this linear relationship is only valid for a nearly Gaussian antenna pattern. In the available literature, based on this relationship the influence of noise measured at the antenna terminals on the bearing error is evaluated. The approach presented in this paper is however different, as the deterministic impact of the lightning rod is evaluated. In the following, analytical estimations on the influence of a metal lightning rod on the antenna pattern are derived.

III. Influence of Lightning Rod

Up to the microwave frequency range, the metal lightning rod can be approximated as a perfect electric conductor that is infinitely extended normal to the azimuthal plane. For a plane wave impinging on such a structure, the Mie scattering theory presents a complete analytical solution for the resulting scattered field. In our approach this scattered field is then assumed superposed to the directly impinging field at the antenna location, thus distorting the effective mounted antenna pattern.

A. Mie Scattering

Early in the development of electromagnetic theory, Mie developed a theory for the scattering of electromagnetic waves on spherical and cylindrical objects [7]. Closed-form expressions of these fields are found e.g. in [8]. Two dual solutions for a TE and TM case were derived. The scattered field strength in the TE case is much larger in magnitude compared to the TM case. For the present application this means the vertically polarized field components are the dominant source of distortion. The scattered field is calculated as [8]

$$E_{scat}(\rho, \Phi) = -E_0 \sum_{n=-\infty}^{\infty} j^{-n} \frac{J_n(kD_0/2)}{H_n^{(2)}(kD_0/2)} H_n^{(2)}(k\rho) e^{-jn\Phi} \tag{5}$$

at a distance ρ and angle Φ from the center of the scattering cylinder. E_0 designates the amplitude of the incident wave and D_0 is the diameter of the metal rod. The incident plane wave has a wavenumber k. The expression contains the Bessel function of the first kind $J_n(x)$ and the second Hankel function $H_n^{(2)}(x)$. The expression (5) consists of an infinite sum, however 20 terms usually yield sufficient accuracy.

B. Superposed Antenna Pattern

In order to estimate the influence of this scattered field on the antenna pattern, far-field conditions are assumed. Furthermore the interaction between the incoming plane wave and the scattered field is assumed to be restricted to a very small area. No diffracted fields around the structure or surface waves are taken into account. The total field at the location of the receiving antenna can be calculated in the geometry of Fig. 2 by superposition of the fields

$$E_{total} = E_{scat}(d_1, \Phi_2) + E_0 e^{-jkd_1 \cos(\Phi_2)} \tag{6}$$

with the first term designating the scattered field at distance d_1 and at angle Φ_2 from the cylinder. The second term takes into account the phase shift for the plane wave while propagating from the metal rod to the receiving antenna. The scattered angle is calculated as

$$\Phi_2 = -(\alpha - \theta) + \Theta_0 + \text{sign}(\Theta_0)\Phi_1. \tag{7}$$

The angle Φ_1 is computed through the law of cosines and Θ_0 designates the angular position of the metal rod.

A new disturbed antenna pattern can now be estimated as [9]

$$D(\alpha) \propto \frac{|E_{total}|^2}{\eta}. \tag{8}$$

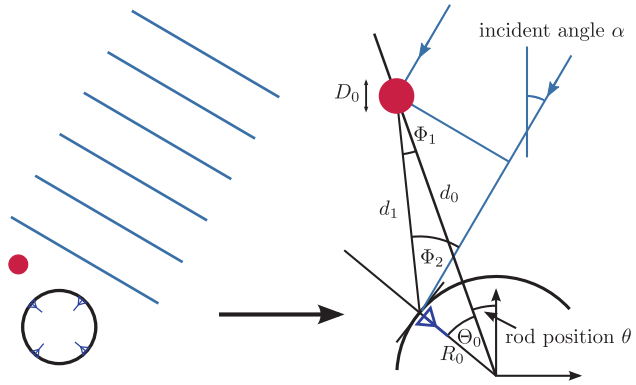

Fig. 2: Calculation of the different angles and positions for a configuration with a rod of diameter D_0 placed at a distance d_0 from the system outer face and at an angle θ from broadside. The DF structure has radius R_0 and the antenna is placed at angle Θ_0. A pulse is impinging at angle α from broadside.

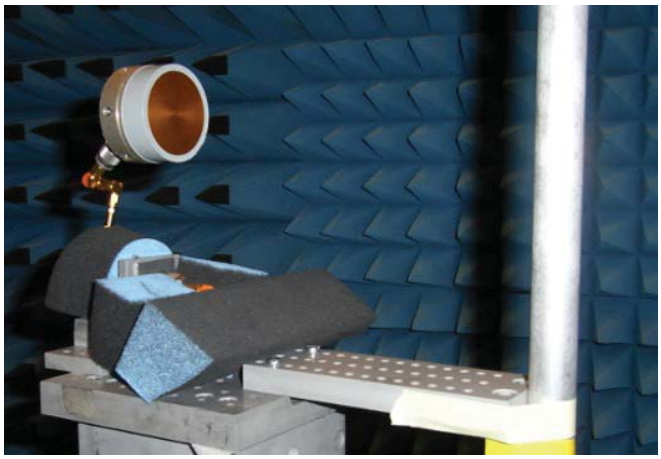

Fig. 3: Experimental setup to evaluate the theoretical model for the distorted antenna parameter.

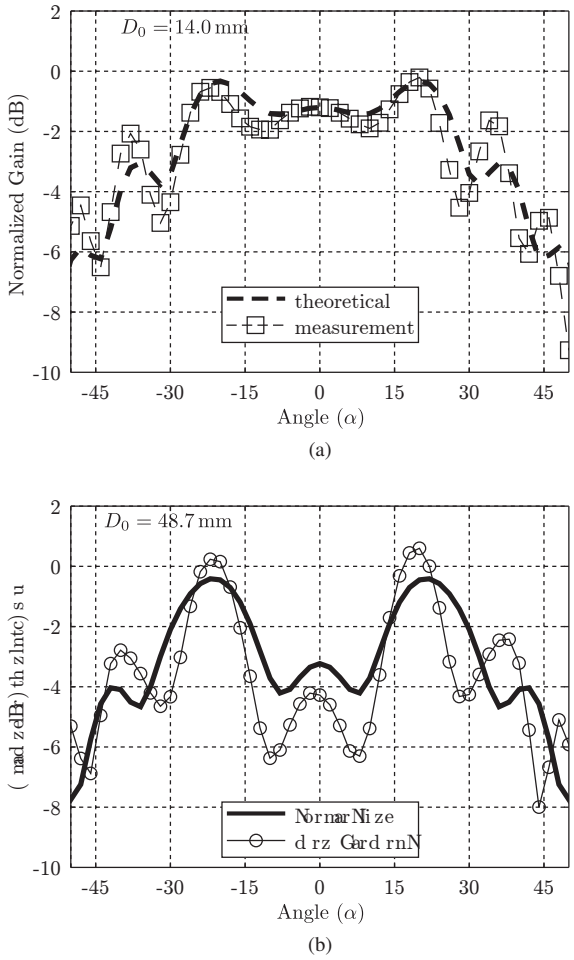

Fig. 4: Comparison between analytical and measured distorted gain normalized to isolated gain for two different rods with a thickness of (a) $D_0 = 14.0\,\mathrm{mm}$ and (b) $D_0 = 48.7\,\mathrm{mm}$ at a frequency of $f = 10\,\mathrm{GHz}$.

In order to evaluate the validity of this formula, measurements have been performed in an idealized setting.

C. Comparison with Measurements

For the sake of simplicity, only the influence of a metal rod in front of the antenna ($\Theta_0 = 0$) was considered for validation. Measurement were performed in an anechoic chamber with several metal rods of different diameters placed in front of a spiral antenna. As reference antenna, a spiral antenna of the same type has been employed. The metal rods were placed at a distance of $d_0 = 22.5\,\mathrm{cm}$, which is typical for practical setups. The experimental arrangement is shown in Fig. 3. A comparison between the expected values (6), (8) and the measured results is shown in Fig. 4. In the analytical model, the value Ψ_0 is set to the measured half-power beamwidth of the receiving spiral. The measured gain in Fig. 4 has been normalized to the undisturbed measured antenna pattern. The thick lines represent the theoretical values, and the marked lines show the measured results. It can be observed that the impact of the scatterer is qualitatively well described by the analytical model. Discrepancies are mainly observed for the larger metal cylinder, for which the far-field assumption becomes less accurate. Generally, the impact of the scatterer is quite conservatively estimated, which means that even larger deviations are to be expected in the final system.

IV. Impact on DF System

Based on the distorted antenna pattern (8) computed with the algorithm introduced in Sec. II, a system consisting of 4 spiral antennas [4] is simulated and the impact of the pattern distortion on the bearing accuracy is evaluated.

First at a frequency of $f = 10\,\mathrm{GHz}$, the influence of the metal rod with a diameter of $D_0 = 48.0\,\mathrm{mm}$ placed at a distance of $d_0 = 22.5\,\mathrm{cm}$ is simulated for a number of rod positions $\Theta_0 = [0°, 25°, 50°, 75°]$. Fig. 5 shows the resulting patterns for a selected angular position. Only the patterns of antennas 1 and 2 are visibly influenced. The

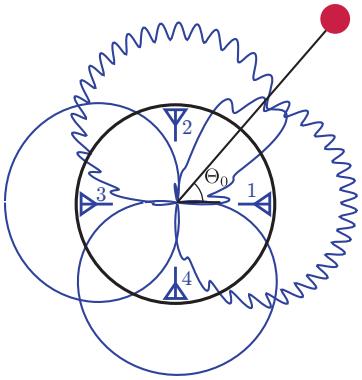

Fig. 5: Example of distorted antenna patterns with a metal rod placed at $\Theta_0 = 50°$.

TABLE I: Parameters as defined in Fig. 2 used in the simulations. The maximum bearing error in this configuration is 9.6°.

frequency f	distance d_0	diameter D_0	angle Θ_0
10 GHz	22.5 cm	4.8 cm	50°

maximum distortion in the disturbed patterns are at different angles than the rod position. This can be explained by the additional angular shift of Φ_2 in the scattered field due to the placement of the metal rod at a distance of the DF system. The oscillations in the pattern are expected to influence the bearing accuracy significantly. In Fig. 6, the bearing error

$$\epsilon(\alpha) = \alpha_{measured} - \alpha \tag{9}$$

is shown for the selected angular positions of the parasitic rod. It is observed that a metal rod placed in front of the antenna ($\Theta_0 = 0$) causes errors of less than 3°. This can be explained by the fact that the error distribution becomes symmetrical, and is canceled out when taking the weighted average of angle measurement obtained with the left and right antenna pair. For other positions, the bearing error can grow up to a significant amount. Interestingly, the impact of the metal rod extends over almost the whole azimuth and generates significant errors far from its angular position. The bearing errors can grow to 12° with $\Theta_0 = 25°$ and $\Theta_0 = 75°$. In practical settings, this will degenerate the system performance significantly.

In a second set of simulations, the maximum absolute error

$$\epsilon_{max} = \max_{\alpha}(|\epsilon(\alpha)|) \tag{10}$$

over the whole azimuth is recorded for specific rod locations. The parameters are set to the values in Table I by default, altering one coefficient at a time. The configuration as given in the table yields a maximum bearing error of $\epsilon_{max} = 9.6°$. First, the angular position Θ_0 of the metal rod is varied. The results are shown in Fig. 7. For positions between 0° and 90°, a symmetric pattern with a minimum at $\Theta_0 = 0°$ is observed. This result is quite non-intuitive, as the metal rod right in front of an antenna could be considered a major error source. Due to the setup of the DoA algorithm though, these errors get mostly

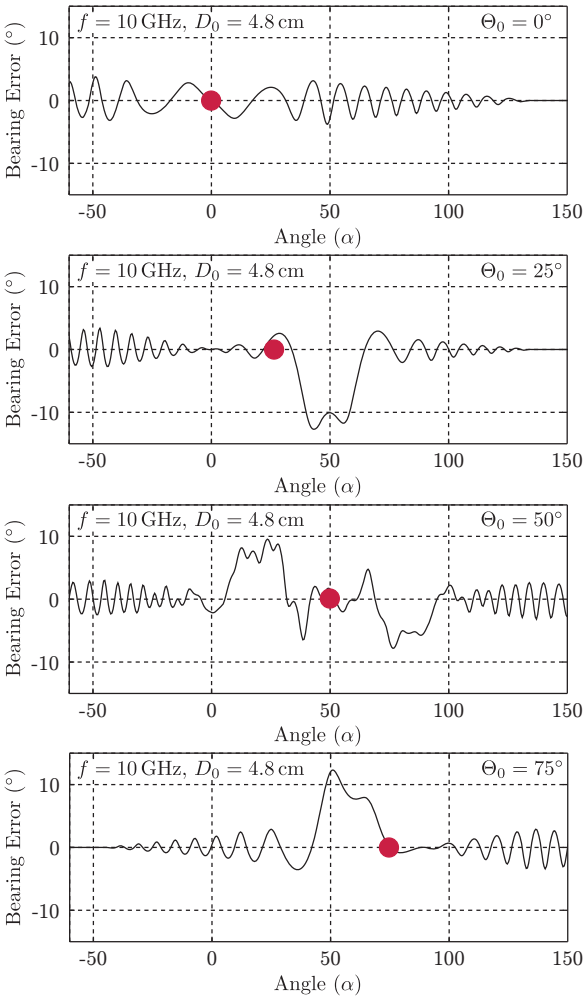

Fig. 6: Bearing error for different angular positions Θ_0 of the metal rod at a frequency of $f = 10$ GHz and at a distance of $d_0 = 22.5$ cm. The red dot indicates the angular location of the rod.

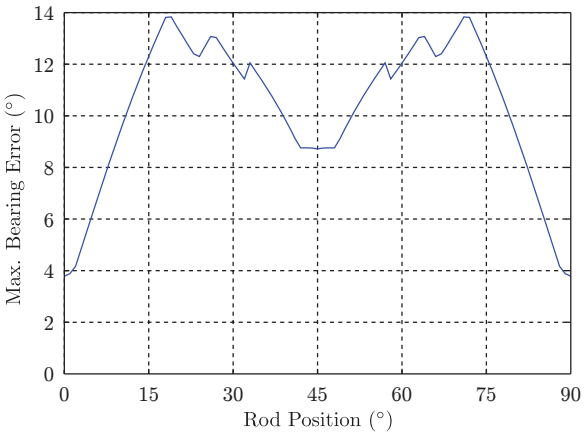

Fig. 7: Maximum bearing error for various angular positions Θ_0 of the metal rod.

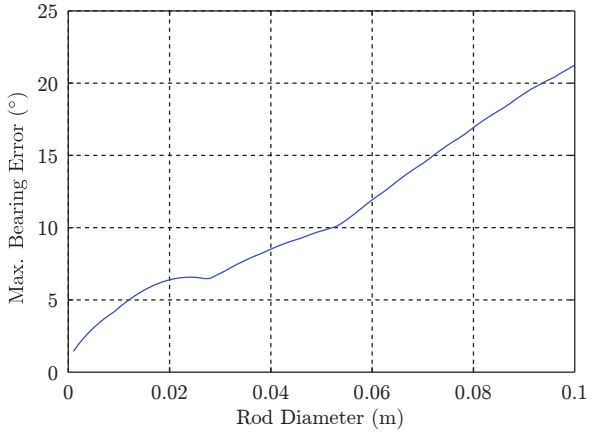

Fig. 8: Maximum bearing error for various diameters D_0 of the metal rod.

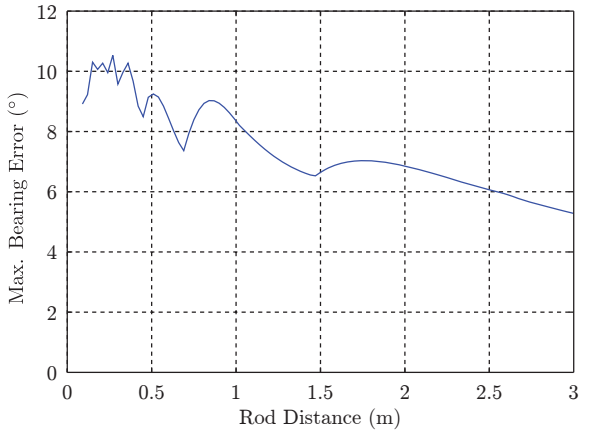

Fig. 9: Maximum bearing error for various distances d_0 between the DF structure and the metal rod.

canceled out as mentioned before. Maximum bearing errors are observed for $\Theta_0 = 18°, 72°$. In these cases, the patterns of both the left and right antenna are significantly disturbed, and the errors of both measurements add up in their average.

The next altered parameter is the diameter of the lightning rod. Fig. 8 shows an almost linear relationship between the bearing error and increasing the rod diameter. The maximum bearing error (10) grows to $\epsilon_{max} = 17°$ for a relatively large diameter of 8 cm.

Furthermore the influence of increasing the distance of the metal rod is investigated in Fig. 9. Intuitively it is expected that the error ϵ_{max} (10) decreases for larger distances. However, practical limitations for efficient lightning protection restrict the possible distance. At distances between $d_0 = 20$ cm and $d_0 = 40$ cm, a maximum of the error is observed. Afterwards, a non-monotonous decline of the error with increasing distances is found. This suggests a manual optimization of the rod position in practical settings.

V. Conclusion

This paper investigated the influence of an external lightning rod on the bearing accuracy of a direction finding system. The algorithm considered here relies on the difference of the amplitudes with a nearly Gaussian antenna pattern of spiral antennas. An analytical model was developed based on the scattering theory from a perfectly conducting cylinder to estimate the distortion in the antenna radiation pattern in the presence of the metal rod. Measurements were employed to confirm the validity of the model.

Due to the simplicity of the analytical model, several parameters could be studied, giving an insight on the impact of the rod on the system. It was found that because of the symmetry of the structure, placing the metal rod directly in front of a antenna minimizes the bearing error. Furthermore, reducing the diameter reduces the bearing error in a nearly linear fashion. Lastly, an increase in the distance proved to significantly reduce the maximum bearing error.

It has been shown that an externally placed lightning rod has a non-negligible influence on the accuracy. It is noted that the analytical model proposed in this paper provides rather conservative estimations of the disturbance caused by the metal rod - in practical settings even larger errors are expected.

In a further study, the influence of different polarizations on the accuracy can give further insight on the influence of the lightning protection strategy in a practical scenario.

Acknowledgement

C. Fumeaux acknowledges the support of the Australian Research Council (ARC) Future Fellowship funding scheme (under FT100100585). The authors would like to express their gratitude to Hansruedi Benedikter from ETH Zurich for the assistance in the experimental setup and measurements.

References

[1] R. G. Wiley, *ELINT : The Interception and Analysis of Radar Signals*. Artech House, 2006.

[2] A. Rembovsky, A. Ashikhmin, V. Kozmin, and S. Smolskiy, *Radio Monitoring: Problems, Methods, and Equipment*, ser. Nanostructure Science and Technology. Springer, 2009, vol. 43.

[3] T. E. Tuncer and B. Friedlander, *Classical and Modern Direction-of-Arrival Estimation*. Academic Press, 2009.

[4] S. Lipsky, *Microwave passive direction finding*. SciTech Publishing, 2004.

[5] C. Fumeaux, D. Baumann, and R. Vahldieck, "Finite-volume time-domain analysis of a cavity-backed archimedean spiral antenna," *Antennas and Propagation, IEEE Transactions on*, vol. 54, no. 3, pp. 844–851, Mar. 2006.

[6] L. Seymour, P. Grant, and C. Cowan, "The effects of sensor positioning errors on bearing estimation," in *Passive Direction Finding, IEE Colloquium on*, Jan. 1989, pp. 9/1–9/8.

[7] G. Mie, "Contributions to the optics of turbid media, particularly of colloidal metal solutions," *Ann. Phys.*, vol. 25, no. 3, pp. 377–445, 1908.

[8] S. Narkimelli and H. Ochoa, "Scattering of electromagnetic radiation for a perfect electric conducting cylinder by using multiple angles of polarization," in *System Theory (SSST), 2010 42nd Southeastern Symposium on*, Mar. 2010, pp. 60–65.

[9] C. Balanis, *Antenna theory*. Wiley New York, 1997.